

---

# Tackling Intertwined Data and Device Heterogeneities in Federated Learning with Unlimited Staleness

---

Haoming Wang and Wei Gao  
University of Pittsburgh  
hm.wang, weigao@pitt.edu

## Abstract

Federated Learning (FL) can be affected by data and device heterogeneities, caused by clients' different local data distributions and latencies in uploading model updates (i.e., staleness). Traditional schemes consider these heterogeneities as two separate and independent aspects, but this assumption is unrealistic in practical FL scenarios where these heterogeneities are intertwined. In these cases, traditional FL schemes are ineffective, and a better approach is to convert a stale model update into a non-stale one. In this paper, we present a new FL framework that ensures the accuracy and computational efficiency of this conversion, hence effectively tackling the intertwined heterogeneities that may cause unlimited staleness in model updates. Our basic idea is to estimate the distributions of clients' local training data from their uploaded stale model updates, and use these estimations to compute non-stale client model updates. In this way, our approach does not require any auxiliary dataset nor the clients' local models to be fully trained, and does not incur any additional computation or communication overhead at client devices. We compared our approach with the existing FL strategies on mainstream datasets and models, and demonstrated that our approach can improve the trained model accuracy by up to 25% and reduce the required amount of training epochs by up to 35%.

## 1 Introduction

Federated Learning (FL) [22] could be affected by data and device heterogeneities. *Data heterogeneity* is the heterogeneity of non-i.i.d. data distributions on different clients, making the aggregated global model biased and reducing model accuracy [14, 36]. *Device heterogeneity* arises from clients' variant latencies in uploading local model updates to the server, due to their different local resource conditions (e.g., computing power, network link speed, etc). An intuitive solution to device heterogeneity is asynchronous FL (AFL), which does not wait for slow clients but updates the global model whenever having received a client update [29]. In this case, a slow client will use an outdated global model to compute its model update, which will be *stale* when aggregated at server and affect model accuracy. To tackle *staleness*, weighted aggregation can be used to apply reduced weights on stale updates [8, 26].

Most existing work considers data and device heterogeneities as two separate and independent aspects in FL [39]. This assumption, however, is unrealistic in many FL scenarios where these two heterogeneities are *intertwined*: data in certain classes or with particular features may only be available at some slow clients. For example, in FL for hazard rescue [2], only devices at hazard sites have crucial data about hazards, but they usually have limited connectivity or computing power to timely upload model updates. Similar situations also happen in FL scenarios where data with high importance to model accuracy is scarce and hard to obtain, e.g., disease evaluation in smart health, where only few patients have severe symptoms but are likely to report symptoms with long delays due to their worsening conditions [9].

In these cases, if reduced weights are applied to stale model updates from slow clients, important knowledge in these updates will not be sufficiently learned and hence affects model accuracy. Instead, a better approach is to equally aggregate all model updates and convert a stale model update into a non-stale one, but existing techniques for such conversion are limited to a small amount of staleness.

For example, first-order compensation can be applied on the gradient delay [38], by assuming that staleness in FL is smaller than one epoch to ignore all the high-order terms in the difference between stale and non-stale model updates [40]. However, in the aforementioned FL scenarios, it is common to witness excessive or even unlimited staleness, and our experiments in Section 2 show that the compensation error will quickly increase when staleness grows.

To efficiently tackle the intertwined data and device heterogeneities with unlimited staleness, in this paper we present a new FL framework that uses gradient inversion at the server to convert stale model updates to non-stale ones, by mimicking the local models’ gradients produced with their original training data [18]. More specifically, the server computes the gradients from clients’ stale model updates to obtain an estimated distribution of clients’ training data, such that a model trained with this estimated data distribution will exhibit a similar loss surface as that of using the clients’ original training data. The server then uses such estimated data distributions to retrain the current global model, as estimations of the clients’ non-stale model updates. Compared to other model conversion methods, such as training an extra generative model [30] or optimizing input data with extra constraints [32], our proposed approach has the following advantages:

- Our approach retains the clients’ FL procedure to be unchanged, and hence does not incur any additional computation or communication overhead at clients, which usually have weak local capabilities in FL scenarios.
- Our approach does not require any auxiliary dataset nor the clients’ local models to be fully trained, and can hence be widely applied to practical FL scenarios.
- In our approach, the server will not be able to recover any original samples of clients’ local training data or produce any recognizable information about such local data. Hence, our approach does not impair the clients’ data privacy.

We evaluated our proposed technique by comparing with the mainstream FL schemes on multiple datasets and models. Experiment results show that when tackling intertwined data and device heterogeneities with unlimited staleness, our technique can significantly improve the trained model accuracy by up to 25% and reduce the required amount of training epochs by up to 35%. Since clients in FL need to compute and upload model updates to the server in every training epoch, such reduction of training epochs largely reduces the computing and communication overhead at clients.

## 2 Related Work and Motivation

In this section, we present preliminary results that show the ineffectiveness of existing FL schemes in tackling intertwined data and device heterogeneities, hence motivating our proposed approach.

### 2.1 Tackling Intertwined Data and Device Heterogeneities in FL

Most existing solutions to staleness in AFL are based on weighted aggregation [8, 26, 7]. For example, [8] suggests that a model update’s weight exponentially decays with its amount of staleness, and some others use different staleness metrics to decide model updates’ weights [26]. [7] decides these weights based on a feature learning algorithm. These existing solutions, however, are improperly biased towards fast clients, and will hence affect the trained model’s accuracy when data and device heterogeneities in FL are intertwined, because they will miss important knowledge in slow clients’ model updates.

To show this, we conducted experiments using a real-world disaster image dataset [23], which contains 6k images of 5 disaster classes (e.g., fires and floods) with different levels of severity. In a FL scenario of 100 clients, we set data heterogeneity as that each client only contain samples in one data class, and set device heterogeneity as a staleness of 100 epochs on 15 clients with images of severe damage. When using this dataset to fine-tune a pre-trained ResNet18 model, results in Figure 1 show that, staleness results in large degradation of model accuracy, and weighted aggregation will further enlarge such degradation.

Some other researchers suggest to use semi-asynchronous FL, where the server either aggregates client model updates at a lower frequency [25] or clusters clients into different asynchronous “tiers” according to their update rates [3]. However, doing so cannot completely eliminate the impact of intertwined data and device heterogeneities, because the server’s aggregation still involves stale model updates.

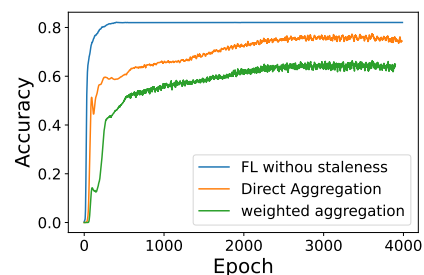


Figure 1: The impact of staleness to AFL with weighted aggregation

Instead, a better approach is to convert stale model updates to unstale ones. Existing techniques on such conversion, such as Asynchronous Stochastic Gradient Descent with Delay Compensation (DC-ASGD) [38], compensate the errors in stale model updates but are only applicable to limited amounts of staleness. As shown in Figure 2, when we increase the amount of staleness from 0 to 60 epochs, DC-ASGD’s first-order compensation error, measured in cosine similarity and L1-norm difference with the unstale model updates, both significantly increase. The basic reason is that higher-order terms in compensation can not be negligible as staleness becomes large. These results motivate us to design better techniques that support accurate conversion with unlimited staleness.

In addition, there are also other existing approaches that transfer knowledge from stale model updates to the global model, by training a generative model and compelling its generated data to exhibit high predictive values on original model updates [31, 20, 42]. One can also optimize the randomly initialized input data until it has good performance on the original model [34]. However, the quality and accuracy of knowledge transfer remain low, and more related experiment results are in Appendix B. Other efforts enhance the quality of knowledge transfer by incorporating natural image priors [21] or using another public dataset to introduce general knowledge [30], but require involvement of extra datasets. Moreover, all these methods require that the clients’ local models to be fully trained, which is usually infeasible in FL.

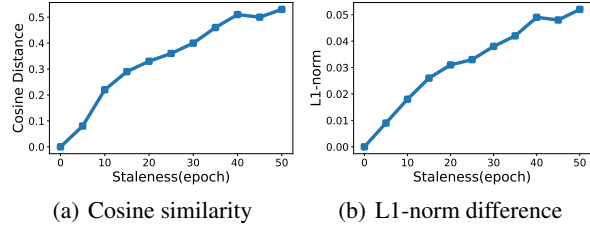


Figure 2: DC-ASGD’s compensation error to staleness in FL

## 2.2 Gradient Inversion

Our approach utilizes gradient inversion [18], which was initially designed to recover the original training data from the gradient of a trained model, by minimizing the difference between the trained model’s gradient and the gradient computed from recovered data. Denote  $x$  as input data samples and  $y$  as labels, gradient inversion solves the following optimization problem:

$$(x'^*, y'^*) = \arg \min_{(x', y')} \left\| \frac{\partial L[(x', y'); w^{t-1}]}{\partial w^{t-1}} - g^t \right\|_2^2, \quad (1)$$

where  $(x', y')$  is the recovered data,  $w^{t-1}$  is the trained model with loss  $L[\cdot]$ , and  $g^t$  is the gradient calculated with  $w^{t-1}$ . This problem can be solved by gradient descent to iteratively update  $(x', y')$ .

The quality of recovered data relates to the amount of data samples recovered. Recovering a larger dataset will confuse the learned knowledge across different samples and hence reduce the quality of recovered data, and existing gradient inversion methods are limited to recovering a very small batch (<48) of data samples [33, 10, 37]. This limitation significantly contradicts with the typical size of clients’ datasets in FL. In this paper, we utilize such contradiction to estimate only the clients’ training data distributions instead of recovering their training data samples. In this way, our approach can minimize the errors in inverse computations and also avoid impairing the clients’ local data privacy.

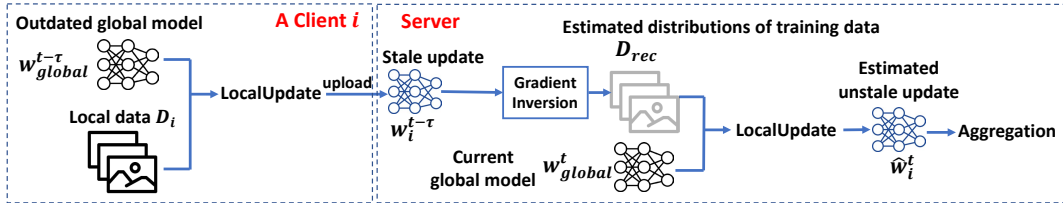


Figure 3: Our proposed method of tackling intertwined data and device heterogeneities in FL

## 3 Method

At time  $t^1$ , a normal client  $i$  in FL provides its model update as

$$w_i^t = LocalUpdate(w_{global}^t; D_i),$$

where  $LocalUpdate[\cdot]$  is client  $i$ ’s local training program, which uses the current global model  $w_{global}^t$  and client  $i$ ’s local dataset  $D_i$  to produce  $w_i^t$ . On the other hand, when the client  $i$ ’s model update is

<sup>1</sup>In the rest of this paper, we use the notation of time  $t$  to indicate the  $t$ -th epoch in FL training.

delayed, the server will receive a stale model update from  $i$  at time  $t$  as

$$w_i^{t-\tau} = \text{LocalUpdate}(w_{global}^{t-\tau}; D_i),$$

where the amount of staleness is  $\tau$  and  $w_i^{t-\tau}$  is computed from an outdated global model  $w_{global}^{t-\tau}$ .

Due to intertwined data and device heterogeneities, we consider that the received  $w_i^{t-\tau}$  contains unique knowledge about  $D_i$  that is only available from client  $i$ , and such knowledge should be sufficiently incorporated into the global model. To do so, as shown in Figure 3, the server uses gradient inversion described in Eq. (1) to compute an intermediate dataset  $D_{rec}$  from  $w_i^{t-\tau}$ . Being different from the existing work of gradient inversion [18] that aims to fully recover the client  $i$ 's local training data  $D_i$ , we only expect  $D_{rec}$  to represent the similar data distribution with  $D_i$ .

The server then computes an estimation of  $w_i^t$  from  $w_i^{t-\tau}$ , namely  $\hat{w}_i^t$ , by using  $D_{rec}$  to train its current global model  $w_{global}^t$ , and aggregates  $\hat{w}_i^t$  with model updates from other clients to update its global model in the current epoch. During this procedure, the server only receives the stale model update  $w_i^{t-\tau}$  from client  $i$ , and we demonstrated that the server's estimation of clients' data distribution will not expose any recognizable information about the clients' local training data, hence avoiding the possible data privacy leakage at clients. At the same time, the computing costs at the client  $i$  remains the same as that in vanilla FL, and no any extra computation is needed for such estimation of  $\hat{w}_i^t$ .

### 3.1 Estimating Local Data Distributions from Stale Model Updates

To compute  $D_{rec}$ , we first fix the size of  $D_{rec}$  and randomly initialize each data sample and label in  $D_{rec}$ . Then, we iteratively update  $D_{rec}$  by minimizing

$$\text{Disparity}[\text{LocalUpdate}(w_{global}^{t-\tau}; D_{rec}), w_i^{t-\tau}], \quad (2)$$

using gradient descent, where  $\text{Disparity}[\cdot]$  evaluates how much  $w_i^{t-\tau}$  changes if being retrained using  $D_{rec}$ . In FL, a client's model update comprises multiple local training steps instead of a single gradient. To use gradient inversion in FL, we substitute the single gradient computed from  $D_{rec}$  in Eq. (1) with the local training outcome using  $D_{rec}$ . In this way, since the loss surface in the model's weight space computed using  $D_{rec}$  is similar to that using  $D_i$ , we can expect a similar gradient being computed. To verify this, we conducted preliminary experiments by using the MNIST dataset to train the LeNet model. Results in Figure 4 show that, the loss surface computed using  $D_{rec}$  is similar to that using  $D_i$  in the proximity of  $(w_{global}^{t-\tau})$ , and the computed gradient is hence very similar, too.

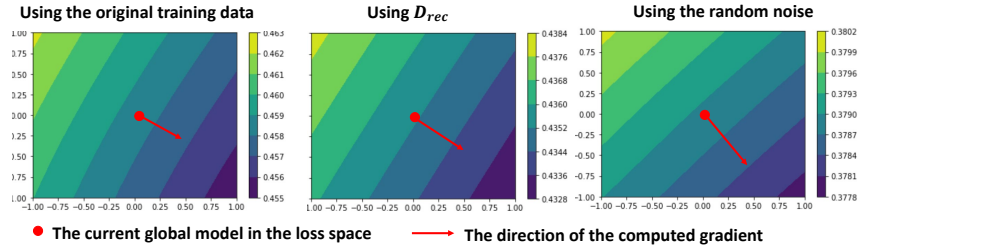


Figure 4: Comparing the loss surface and gradient computed using  $D_{rec}$ ,  $D_i$ , and random noise data

To verify the accuracy of using  $\hat{w}_i^t$  to estimate  $w_i^t$ , we compare this estimation with DC-ASGD's first-order estimation, by computing their discrepancies with the true unstale model update under different amounts of staleness, using the MNIST dataset and LeNet model. Results in Figure 5 show that, compared to DC-ASGD's first-order estimation, our estimation based on gradient inversion can reduce the estimation error by up to 50%, especially when the amount of staleness excessively increases to more than 50 epochs.

Another key issue is how to decide the size of  $D_{rec}$ . Since gradient inversion is equivalent to data resampling in the original training data's distribution, a sufficiently large size of  $D_{rec}$  is necessary to ensure unbiased data sampling and sufficient minimization of gradient loss through iterations. On the other hand, when the size of  $D_{rec}$  is too large, the computational overhead of each iteration would be unnecessarily too high. We will provide more technical details about how to decide the size of  $D_{rec}$  in Appendix A.

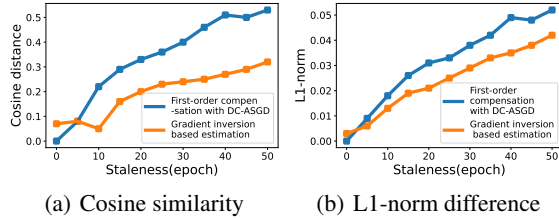


Figure 5: Our method of gradient inversion based estimation has smaller error compared to that of DC-ASGD's estimation

### 3.2 Switching back to Vanilla FL in Later Stages of FL Training

As shown in Figure 5, the estimation made by gradient inversion always contains errors. As the FL training progresses and the global model converges, the difference between stale and unstale model updates diminishes, implying that in the late stage of FL, the error in our estimated model update ( $\hat{w}_i^t$ ) will exceed that of the original stale model update  $w_i^{t-\tau}$ . To verify this, we conducted experiments by training the LeNet model with the MNIST dataset, and evaluated the average values of  $E_1(t) = \text{Disparity}[\hat{w}_i^t; w_i^t]$  and  $E_2(t) = \text{Disparity}[w_i^{t-\tau}; w_i^t]$  across different clients, using both cosine similarity and L1-norm difference as the metric. Results in Figure 6 show that at the final stage of FL training,  $E_2(t)$  is always larger than  $E_1(t)$ .

Hence, in the late stage of FL training, it is necessary to switch back to vanilla FL and directly use stale model updates in aggregation. The difficulty of deciding such switching point is that the true unstale model update ( $w_i^t$ ) is unknown at time  $t$ . Instead, the server will be likely to receive  $w_i^t$  at a later time, namely  $t + \tau'$ . Therefore, if we found that  $E_1(t) > E_2(t)$  at time  $t + \tau'$  when the server receives  $w_i^t$  at  $t + \tau'$ , we can use  $t + \tau'$  as the switching point instead of  $t$ . Doing so will result in a delay in switching, but our experiment results in Figure 7 with different switching points show that the FL training is insensitive to such delay.

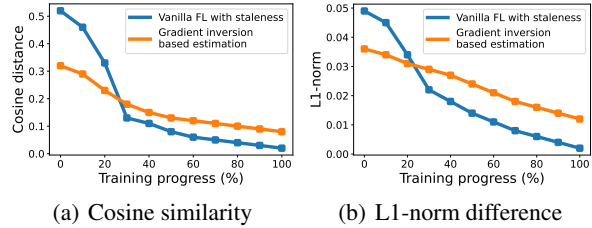
In practice, when we make such switch, the model accuracy in training will experience a sudden drop, as shown in Figure 7, due to the inconsistency of gradient between  $\hat{w}_i^t$  and  $w_i^{t-\tau}$ . To avoid such drop, at time  $t + \tau'$ , instead of immediately switching to using  $\hat{w}_i^t$  in server's model aggregation, we use a weighted average of  $\alpha\hat{w}_i^t + (1 - \alpha)w_i^{t-\tau}$  in aggregation, so as to ensure smooth switching.

### 3.3 Reducing the Computing Cost of Gradient Inversion

Our design retains the clients' FL procedure to be unchanged, and offload all the extra computations incurred by gradient inversion to the server. Then, we reduce the server's computing cost of gradient inversion, which is caused by the large amount of iterations involved, using the following two methods.

First, we reduce complexity of the objective function in gradient inversion by sparsification, which only involves the important gradients with large magnitudes into iterations. Existing work has verified that gradients in mainstream models are highly sparse and only few gradients have large magnitudes [19]. Hence, we use a binary mask to selecting elements in  $w_i^{t-\tau}$  with the top- $K$  magnitudes and only involve these elements to gradient inversion. As shown in Figure 8(a), by only involving the top 5% of gradients, we can reduce around 80% of iterations in gradient inversion, with with slight increase in the error of estimating unstale model updates.

Second, since in most FL scenarios the clients' local training data remains fixed, we do not need to start iterations of gradient inversion every time from a random initialization, but could instead optimize  $D_{rec}$  from those calculated in the previous training epochs. Our experiments in Figure 8(b) show that, when the clients' local training data remains fixed, we can further reduce the amount of iterations in gradient inversion by another 43%. Even if such client data is only partially fixed, we can still achieve non-negligible reduction of such iterations.



(a) Cosine similarity (b) L1-norm difference  
Figure 6: Comparison of model updates' estimation error as the FL training progresses

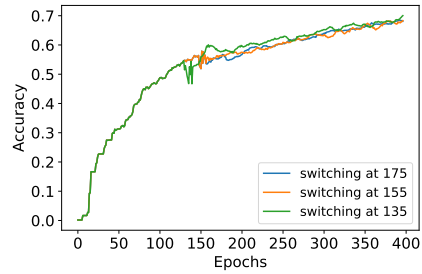
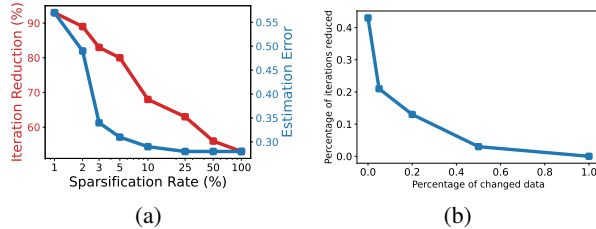


Figure 7: FL training results with different switching points.  $E_1(t) > E_2(t)$  when  $t=155$ , but different switching points exhibit very similar training performance.



(a) (b)  
Figure 8: Computing cost reduction: (a) Number of iterations in gradient inversion with different sparsification rates. (b) Number of iterations in gradient inversion with different percentages of changes in clients' local data. MNIST dataset and LeNet model are used.

### 3.4 Addressing the Possible Privacy Leakage due to Data Estimation

Using gradient inversion to recover local data distributions from clients’ model updates may impair the clients’ data privacy. To avoid such possible privacy leakage, we aim to ensure that our estimation algorithms in Section 3.1 do not recover any recognizable information about clients’ local data.

As stated in Section 2.2, although our estimation algorithm is similar to [18] as a weak inversion attack, its attacking power depends on the amount of data samples to be recovered. In FL, a client’s local training data usually contains at least hundreds of samples [27], and the high diversity among data samples make it difficult to precisely recover any individual sample. To show this, we did experiments with CIFAR-10 dataset and ResNet-18 model, and match each sample in  $D_{rec}$  with the most similar sample in  $D_i$  based on their LPIPS similarity score [35]. As shown in Figure 9, these matching data samples are highly dissimilar, and recovered data samples in  $D_{rec}$  are mostly meaningless in human perception.

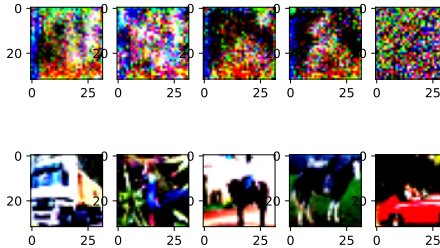
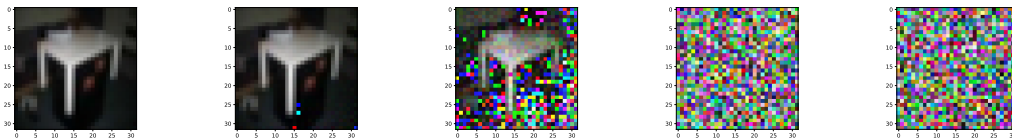


Figure 9: The five best matches between samples in  $D_{rec}$  and  $D_i$ . The top row represents samples in  $D_{rec}$ , and the bottom row represents samples in  $D_i$ .

Besides, in extreme scenarios where client’s local training data only contains very few data samples and client’s local model is only trained for one step, gradient inversion’s attacking power is sufficient to recover the training samples [10]. In these cases, our sparsification approach described in Section 3.3 can be used to mitigate such attacking power and protect clients’ data privacy, as also suggested in [18], because sparsification effectively reduces the scope of knowledge available in gradient inversion for data recovery. To show this, we use LeNet and ResNet18 in FL and only 1 data sample in CIFAR-10 as the local training data, and then repeatedly use gradient inversion for data recovery until the recovered image quality never improves further.

Metric	Model	0%	30%	95%	Random Noise
MSE ↓	LeNet	5e-4	0.014	2.75	1.12
	ResNet18	0	0.011	3.16	1.12
PSNR ↑	LeNet	261	155	41.8	47.8
	ResNet18	323	218	43.3	47.8
LPIPS [35] ↓	LeNet	0	0.04	0.56	0.50
	ResNet18	0	0.01	0.59	0.50
FID [12] ↓	LeNet	0	57	391	489
	ResNet18	0	48	433	489

Table 1: Quality of data recovery with different sparsification rates. Different metrics are used to measure the similarity between recovered and original data samples.



(a) Original image (b) 0% sparsification (c) 30% sparsification (d) 95% sparsification (e) Random noise

Figure 10: Recovered images under different sparsification rates

As shown in Table 1, when sparsification rate is 95% as suggested in Section 3.2, images recovered by gradient inversion are very dissimilar with the original data samples. In particular, when being measured by perceptual image quality metrics such as LPIPS and FID, such dissimilarity is at the same level with that between random noise and original data samples. Such dissimilarity is further illustrated in Figure 10, where the images recovered with 95% sparsification rate is similar to random noise. These results demonstrate that, even in FL scenarios that allow the maximum attacking power, our sparsification approach can still ensure that gradient inversion does not expose any recognizable information about clients’ local training data, with the minimum impact on FL performance.

Defense	None	95% sparsification	95% sparsification + noise
Accuracy of label recovery	85.5%	66.7%	46.4%

Table 2: Accuracy of label recovery

In addition, labels may also be inferred by gradient inversion. We evaluate such risk by measuring the accuracy of label recovery under the same setting. As show in Table2, by applying 95% sparification rate and adding noise to clients’ model updates, we can reduce the accuracy of label recovery to <50%.

### 3.5 Addressing the Possible Privacy Leakage of Clients’ Data Labels

To preserve the clients’ data privacy, our approach should not require clients to upload or reveal any extra information to the server, other than uploading their local model updates as they do in vanilla FL. However, as described in Section 3.2, our approach should only be applied to stale clients when data and device heterogeneities are intertwined, i.e., these clients’ local data is unique and unavailable elsewhere. To properly decide such uniqueness, the server will need to know the class labels of clients’ data, hence impairing the clients’ local data privacy.

To address this problem, we instead decide such uniqueness with a new algorithm at the server, which compares the directions of stale clients’ model updates with those of unstale clients’ model updates, and only consider stale clients’ data as unique if such difference is sufficiently large. In this way, we do not require any information about clients’ data labels to be uploaded to the server.

We quantify such difference between model updates  $w_i^t$  and  $w_j^t$  using the cosine distance, such that

$$D_c(w_i^t, w_j^t) = 1 - \frac{w_i^t \cdot w_j^t}{\|w_i^t\| \|w_j^t\|}, \quad (3)$$

and the threshold is computed as the average of cosine distances between unstale model updates at  $t - \tau$ . Since the scale of cosine distance changes during FL training [17], such averaging can add some adaptivity to the threshold.

We conducted preliminary experiments to evaluate if the server can accurately decide the uniqueness of clients’ local data, by assigning each client with data samples from one random class. Results in Figure 11 show that the accuracy quickly grows to >90% as training progresses, and the average accuracy is 93%.

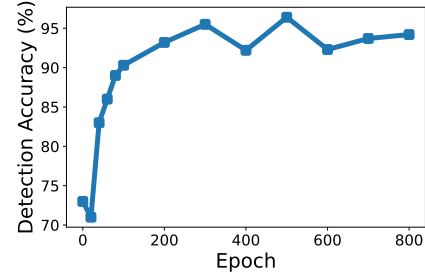


Figure 11: Accuracy of deciding the uniqueness of clients’ local data

## 4 Experiments

We evaluated our technique in two FL scenarios. First, all clients’ local datasets are fixed. Second, we consider a more practical FL setting, where clients’ local data is continuously updated and data distributions are variant over time, due to dynamic changes of environmental contexts. We compare our technique with the following baselines that tackle stale model updates:

- **Direct aggregation (Baseline 1):** Directly aggregating stale model updates without weights.
- **Weighted aggregation (Baseline 2):** Applying weights onto stale model updates in aggregation, and these weights are inversely proportional to the amount of staleness [8].
- **First-order compensation (Baseline 3):** Compensating errors in stale model updates using first-order Taylor expansion and Hessian approximation [38, 41].
- **Future model prediction (Baseline 4):** Assuming staleness as pre-known, the future global model is predicted by first-order method above and used to compensate stale updates [11].
- **FL with asynchronous tiers (Baseline 5):** It clusters clients into asynchronous tiers based on staleness and uses synchronous FL in each tier [4].

In addition, we also compared our technique with standard FL without staleness, referred as “Unstale” in figures, to assess the disparity between estimations and true values of unstale updates and the true value of unstale updates.

### 4.1 Experiment Setup

In all experiments, we consider a FL scenario with 100 clients. Each local model update on a client is trained by 5 epochs using the SGD optimizer, with a learning rate of 0.01 and momentum of 0.5.

To emulate data heterogeneity, we use a Dirichlet distribution to sample client datasets with different label distributions [13], and use a tunable parameter ( $\alpha$ ) to adjust the amount of data heterogeneity: as shown in Figure 12, the smaller  $\alpha$  is, the more biased these label distributions will be and hence the

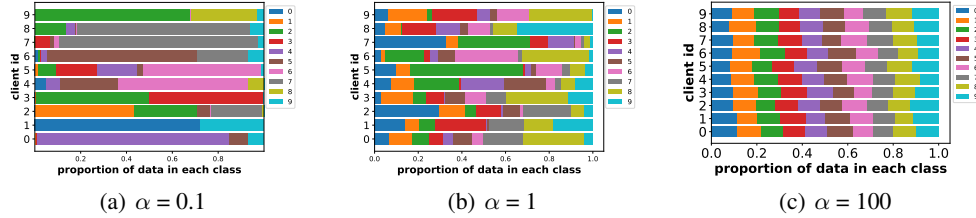


Figure 12: Emulating data heterogeneity using Dirichlet Distribution. Data distributions on 10 clients are shown.

higher amount of data heterogeneity exists. When  $\alpha$  is very small, the local dataset of each client only contains data samples of few data classes.

To emulate device heterogeneity intertwined with data heterogeneity, we select one data class to be affected by staleness, and apply different amounts of staleness, measured by the number of epochs that clients’ model updates are delayed, to the top 10 clients whose local datasets contain the most data samples of the selected data class. The impact of staleness, on the other hand, can be further enlarged by applying staleness in the similar way to more data classes.

Based on such experiment setup, we evaluate the FL performance as the trained model’s accuracy in the selected data class affected by staleness. We expect that our approach can either improve the model accuracy, or achieve the same level of model accuracy with baselines but use fewer training epochs.

#### 4.2 FL Performance in the Fixed Data Scenario

In the fixed data scenario, 3 standard datasets and 1 domain-specific dataset are used in FL:

- Using the MNIST [16] and FMNIST [28] datasets to train a LeNet model;
- Using CIFAR-10 [15] dataset to train a ResNet-18 model;
- Using a disaster image dataset MDI [23] to fine-tune the fully connected layers of a ResNet-18 model pre-trained with ImageNet.

The trained model’s accuracies using different FL schemes, with the amount of staleness as 40 epochs, are listed in Table 3. The training progresses of first-order compensation (Baseline 3) and future global weights prediction (Baseline 4) closely resemble that of direct aggregation (Baseline 1), suggesting that estimating stale model updates with Taylor expansion is ineffective under unlimited staleness. Similarly, weighted aggregation (Baseline 2) will lead to a biased model with much lower accuracy. In contrast, our gradient inversion based compensation can improve the trained model’s accuracy by at least 4%, compared to the best baseline. Such advantage in model accuracy can be as large as 25% when compared with weighted aggregation (Baseline 2).

Accuracy(%)	MNIST	FMNIST	CIFAR10	MDI
Direct aggregation (Baseline 1)	57.4	49.2	22.8	72.3
Weighted aggregation (Baseline 2)	39.2	30.1	12.6	61.2
First-order compensation (Baseline 3)	57.4	49.3	22.6	72.3
Future global weights prediction (Baseline 4)	57.3	48.9	22.9	72.2
FL with asynchronous tiers (Baseline 5)	57.6	50.3	25.9	69.8
Ours	<u>61.2</u>	<u>55.4</u>	<u>29.4</u>	<u>75.4</u>

Table 3: Accuracy of the trained model with different datasets in the fixed data scenario

Figure 13 further show the FL training procedure over different epochs, and demonstrated that our proposed technique can also improve the progress and stability of training, and achieve higher model accuracy during different stages of FL training.

Furthermore, we also conducted experiments with different amounts of data and device heterogeneity, using MNIST dataset and LeNet model. Results in Figure 14 and 15 show that<sup>2</sup>, compared with baselines, our technique can generally achieve higher model accuracy or reach the same accuracy with fewer training epochs, especially when the amount of staleness is large.

#### 4.3 FL Performance in the Variant Data Scenario

<sup>2</sup>The model accuracies of Baseline 1, 3 and 4 are very similar, and hence overlap with each other in the figures.



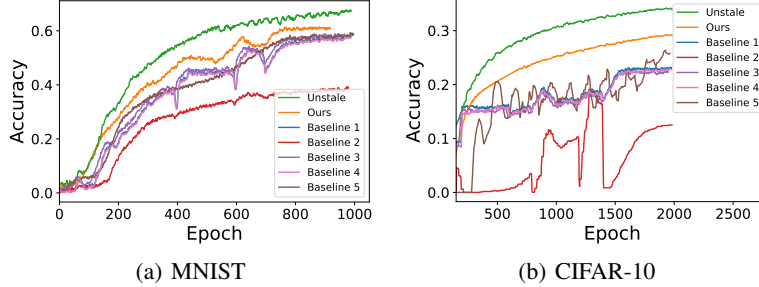
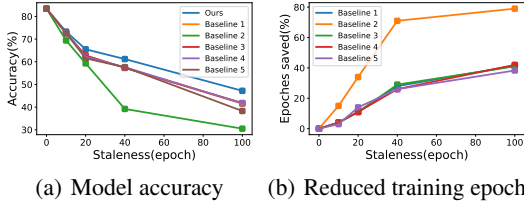
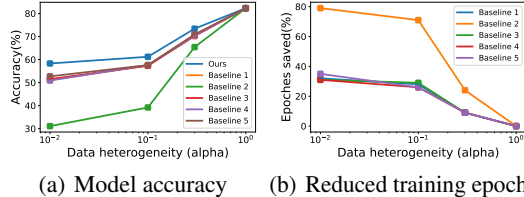


Figure 13: The FL training procedure in data class 5 affected by staleness, using the MNIST dataset to train a LeNet model and the CIFAR-10 dataset to train a ResNet-18 model



(a) Model accuracy (b) Reduced training epochs

Figure 14: The trained model accuracy and percentage of training epochs saved, with different amounts of staleness measured in the number of delayed epochs



(a) Model accuracy (b) Reduced training epochs

Figure 15: The trained model accuracy and percentage of training epochs saved, with different amounts of data heterogeneity controlled by in the Dirichlet distribution

To continuously vary the data distributions of clients' local datasets, we use two public datasets, namely MNIST and SVHN [24], which are for the same learning task (i.e., handwriting digit recognition) but with different feature representations as shown in Figure 16. Each client's local dataset is initialized as the MNIST dataset in the same way as in the fixed data scenario. Afterwards, during training, each client continuously replaces random data samples in its local dataset with new data samples in the SVHN dataset.



Figure 16: Datasets for digit recognition: MNIST and SVHN

Experiment results in Figure 17 show that in such variant data scenario, since clients' local data distributions continuously change, the FL training will never converge. Hence, the model accuracy achieved by the existing FL schemes exhibited significant fluctuations over time and stayed low (<40%). In comparison, our technique can better depict the variant data patterns and hence achieve much higher model accuracy, which is comparable to FL without staleness and 20% higher than those in existing FL schemes.

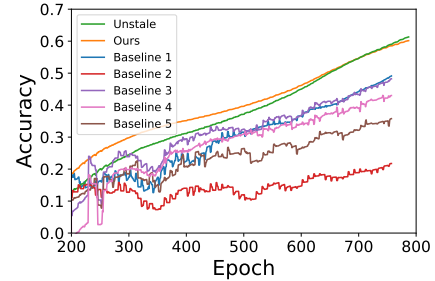
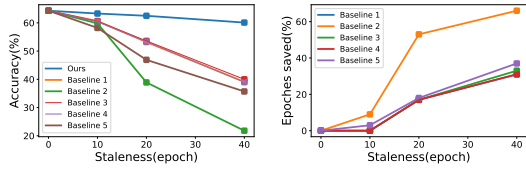


Figure 17: Model accuracy with variant data distributions in clients' local datasets

In addition, we also conducted experiments with different amounts of staleness and different rates of data distribution variations. We apply different variation rates of clients' local data distributions by replacing different amounts of such random data samples in the clients' local datasets in each epoch. To prevent the training from stopping too early when the variation rate is high, we repeatedly varied the data when the variation rate exceeded 1 sample per epoch. Results in Figure 18 and Figure 19 demonstrated that our proposed method outperformed the existing FL schemes, especially when the variation rate is large. Baselines 1, 3, 4, and 5 show similar performance since they cannot compensate such large staleness, and Baseline 2 performs the worst since weighted aggregation leads the model to bias toward other unstable clients.

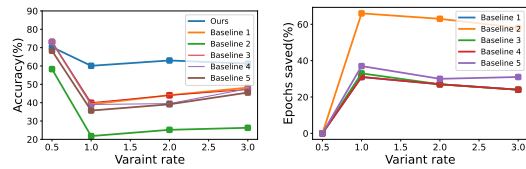
## 5 Conclusion

In this paper, we present a new FL framework to tackle the intertwined data and device heterogeneities in FL, by using gradient inversion to compute non-stale model updates from clients' stale model updates. Experiment results show that our technique can largely improve the model accuracy and reduce the amount of training epochs needed.



(a) Model accuracy (b) Reduced training epochs

Figure 18: The trained model accuracy and the number of training epochs reduced, with different amounts of staleness measured in the number of delayed epochs.



(a) Model accuracy (b) Reduced training epochs

Figure 19: The trained model accuracy and epochs saved compared with baselines with different rates of clients' data variation

## References

- [1] e. a. Addepalli, Sravanti. Degan: Data-enriching gan for retrieving representative samples from a trained classifier.. In *Proceedings of the AAAI Conference on Artificial Intelligence*, 2020.
- [2] L. Ahmed, K. Ahmad, N. Said, B. Qolomany, J. Qadir, and A. Al-Fuqaha. Active learning based federated learning for waste and natural disaster image classification. *IEEE Access*, 8: 208518–208531, 2020.
- [3] e. a. Chai, Zheng. FedAT: A high-performance and communication-efficient federated learning system with asynchronous tiers. In *Proceedings of the International Conference for High Performance Computing, Networking, Storage and Analysis*, 2021.
- [4] Z. Chai, Y. Chen, A. Anwar, L. Zhao, Y. Cheng, and H. Rangwala. Fedat: A high-performance and communication-efficient federated learning system with asynchronous tiers. In *Proceedings of the International Conference for High Performance Computing, Networking, Storage and Analysis*, pages 1–16, 2021.
- [5] e. a. Charpiat, Guillaume. Input similarity from the neural network perspective. In *Advances in Neural Information Processing Systems 32*, 2019.
- [6] e. a. Chen, Hanting. Data-free learning of student networks. In *Proceedings of the IEEE/CVF international conference on computer vision*, 2019.
- [7] e. a. Chen, Yujing. Asynchronous online federated learning for edge devices with non-iid data. In *2020 IEEE International Conference on Big Data (Big Data)*, 2020.
- [8] X. S. Chen, Yang and Y. Jin. Communication-efficient federated deep learning with layerwise asynchronous model update and temporally weighted aggregation. In *IEEE transactions on neural networks and learning systems*, 2019.
- [9] Y. Chen, X. Yang, B. Chen, C. Miao, and H. Yu. Pdassist: Objective and quantified symptom assessment of parkinson's disease via smartphone. In *2017 IEEE International Conference on Bioinformatics and Biomedicine (BIBM)*, pages 939–945. IEEE, 2017.
- [10] e. a. Geiping, Jonas. Inverting gradients-how easy is it to break privacy in federated learning? In *Advances in Neural Information Processing Systems 33*, 2020.
- [11] I. Hakimi, S. Barkai, M. Gabel, and A. Schuster. Taming momentum in a distributed asynchronous environment. *arXiv preprint arXiv:1907.11612*, 2019.
- [12] M. Heusel, H. Ramsauer, T. Unterthiner, B. Nessler, and S. Hochreiter. Gans trained by a two time-scale update rule converge to a local nash equilibrium. *Advances in neural information processing systems*, 30, 2017.
- [13] H. Q. Hsu, Tzu-Ming Harry and M. Brown. Measuring the effects of non-identical data distribution for federated visual classification. In *arXiv preprint*, 2019.
- [14] e. a. Konečný, Jakub. Federated optimization: Distributed machine learning for on-device intelligence. In *arXiv preprint arXiv:1610.02527*, 2016.
- [15] a. G. H. Krizhevsky, Alex. *Learning multiple layers of features from tiny images*. 2009.

- [16] C. C. LeCun, Yann and C. Burges. Mnist handwritten digit database. <http://yann.lecun.com/exdb/mnist>, 2010.
- [17] Z. Li, T. Lin, X. Shang, and C. Wu. Revisiting weighted aggregation in federated learning with neural networks. *arXiv preprint arXiv:2302.10911*, 2023.
- [18] Z. L. Ligeng Zhu and S. Han. Deep leakage from gradients. In *Advances in neural information processing systems 32*, 2019.
- [19] Y. Lin, S. Han, H. Mao, Y. Wang, and W. J. Dally. Deep gradient compression: Reducing the communication bandwidth for distributed training. *arXiv preprint arXiv:1712.01887*, 2017.
- [20] R. G. Lopes, S. Fenu, and T. Starner. Data-free knowledge distillation for deep neural networks. *arXiv preprint arXiv:1710.07535*, 2017.
- [21] e. a. Luo, Liangchen. Large-scale generative data-free distillation. In *arXiv preprint arXiv:2012.05578*, 2020.
- [22] e. a. McMahan, Brendan. Communication-efficient learning of deep networks from decentralized data. In *arXiv preprint*, 2016.
- [23] H. Mouzannar, Y. Rizk, and M. Awad. Damage identification in social media posts using multimodal deep learning. In *ISCRAM*. Rochester, NY, USA, 2018.
- [24] e. a. Netzer, Yuval. Reading digits in natural images with unsupervised feature learning. In *Advances in Neural Information Processing Systems 32*, 2011.
- [25] e. a. Nguyen, John. Federated learning with buffered asynchronous aggregation. In *International Conference on Artificial Intelligence and Statistics. PMLR*, 2022.
- [26] e. a. Wang, Qiyuan. AsyncFedED: Asynchronous Federated Learning with Euclidean Distance based Adaptive Weight Aggregation. In *arXiv preprint*, 2022.
- [27] J. Wang, Z. Charles, Z. Xu, G. Joshi, H. B. McMahan, M. Al-Shedivat, G. Andrew, S. Avestimehr, K. Daly, D. Data, et al. A field guide to federated optimization. *arXiv preprint arXiv:2107.06917*, 2021.
- [28] H. Xiao, K. Rasul, and R. Vollgraf. Fashion-mnist: a novel image dataset for benchmarking machine learning algorithms. *arXiv preprint arXiv:1708.07747*, 2017.
- [29] S. K. Xie, Cong and I. Gupta. Asynchronous federated optimization. In *arXiv preprint*, 2019.
- [30] e. a. Yang, Ziqi. Neural network inversion in adversarial setting via background knowledge alignment. In *Proceedings of the 2019 ACM SIGSAC Conference on Computer and Communications Security*, 2019.
- [31] e. a. Ye, Jingwen. Data-free knowledge amalgamation via group-stack dual-gan. In *Proceedings of the IEEE/CVF Conference on Computer Vision and Pattern Recognition*, 2020.
- [32] e. a. Yin, Hongxu. Dreaming to distill: Data-free knowledge transfer via deepinversion. In *Proceedings of the IEEE/CVF Conference on Computer Vision and Pattern Recognition*, 2020.
- [33] e. a. Yin, Hongxu. See through gradients: Image batch recovery via gradinversion. In *Proceedings of the IEEE/CVF Conference on Computer Vision and Pattern Recognition*, 2021.
- [34] e. a. YYin, Hongxu. Dreaming to distill: Data-free knowledge transfer via deepinversion. In *Proceedings of the IEEE/CVF Conference on Computer Vision and Pattern Recognition*, 2020.
- [35] e. a. Zhang, Richard. The unreasonable effectiveness of deep features as a perceptual metric. In *Proceedings of the IEEE conference on computer vision and pattern recognition*, 2018.
- [36] e. a. Zhao, Yue. Federated learning with non-iid data. In *arXiv preprint*, 2018.
- [37] K. R. M. Zhao, Bo and H. Bilen. idlg: Improved deep leakage from gradients. In *arXiv preprint arXiv:2001.02610*, 2020.

- [38] S. Zheng, Q. Meng, T. Wang, W. Chen, N. Yu, Z.-M. Ma, and T.-Y. Liu. Asynchronous stochastic gradient descent with delay compensation. In *International Conference on Machine Learning*, pages 4120–4129. PMLR, 2017.
- [39] e. a. Zhou, Chendi. TEA-fed: time-efficient asynchronous federated learning for edge computing. In *Proceedings of the 18th ACM International Conference on Computing Frontiers*, 2021.
- [40] Q. Y. Zhou, Yuhao and J. Lv. Communication-efficient federated learning with compensated overlap-fedavg. In *IEEE Transactions on Parallel and Distributed Systems*, 2021.
- [41] H. Zhu, J. Kuang, M. Yang, and H. Qian. Client selection with staleness compensation in asynchronous federated learning. *IEEE Transactions on Vehicular Technology*, 72(3):4124–4129, 2022.
- [42] Z. Zhu, J. Hong, and J. Zhou. Data-free knowledge distillation for heterogeneous federated learning. In *International conference on machine learning*, pages 12878–12889. PMLR, 2021.

## A Deciding the Proper Size of $D_{rec}$

In our proposed approach to estimating the clients’ local data distributions from stale model updates described in Section 3.1, a key issue is how to decide the proper size of  $D_{rec}$ . Since gradient inversion is equivalent to data resampling in the original training data’s distribution, a sufficiently large size of  $D_{rec}$  would be necessary to ensure unbiased data sampling and sufficient minimization of gradient loss through iterations. On the other hand, when the size of  $D_{rec}$  is too large, the computational overhead of each iteration would be unnecessarily too high.

We experimentally investigated such tradeoff by using the MNIST and CIFAR-10 [15] datasets to train a LeNet model. Results in Tables 4 and 5, where the size of  $D_{rec}$  is represented by its ratio to the size of original training data, show that when the size of  $D_{rec}$  is larger than 1/2 of the size of the original training data, further increasing the size of  $D_{rec}$  only results in little extra reduction of the gradient inversion loss but dramatically increase the computational overhead. Hence, we believe that it is a suitable size of  $D_{rec}$  for FL. Considering that clients’ local dataset in FL contain at least hundreds of samples, we expect a big size of  $D_{rec}$  in most FL scenarios.

Size	1/64	1/16	1/4	1/2	2	10
Time(s)	193	207	214	219	564	2097
GI loss	27	4.1	2.56	1.74	1.62	1.47

Table 4: Tradeoff between gradient inversion (GI) loss and computing time with different sizes of  $D_{rec}$  after 15k iterations, with the MNIST dataset

Size	1/64	1/16	1/4	1/2	2	10
Time(s)	423	440	452	474	1330	4637
GI Loss	1.97	0.29	0.16	0.15	0.15	0.12

Table 5: Tradeoff between gradient inversion (GI) loss and computing time with different sizes of  $D_{rec}$  after 15k iterations, with the CIFAR-10 dataset

Such a big size of  $D_{rec}$  directly decides our choice of how to evaluate the change of  $w_i^{t-\tau}$  in Eq. (2). Most existing works use cosine similarity between  $LocalUpdate(w_{global}^{t-\tau}; D_{rec})$  and  $w_i^{t-\tau}$  to evaluate their difference in the direction of gradients, so as to maximize the quality of individual data samples in  $D_{rec}$  [5]. However, since we aim to compute a large  $D_{rec}$ , this metric is not applicable, and instead we use L1-norm as the metric to evaluate how using  $D_{rec}$  to retrain  $w_{global}^{t-\tau}$  will change its magnitude of gradient, to make sure that  $D_{rec}$  incurs the minimum impact on the state of training.

## B Other Approaches to Data Knowledge Estimation

Our basic approach in this paper is to use the gradient inversion technique [18] to estimate knowledge about the clients’ local training data from their uploaded stale model updates, and then use such estimated knowledge to compute the corresponding non-stale model updates for aggregation in FL. In this appendix, we provide supplementary justifications about the ineffectiveness of other methods for such data knowledge estimation, hence better motivating our proposed design.



Figure 20: The computed data samples, when being averaged, can represent a blurred image that matches the data pattern in the original dataset (i.e., handwriting digits in the MNIST dataset)

Method	GI based estimation	direct aggregation	using samples from generative model
Estimation error	0.32	0.52	0.86

Table 6: Error of estimating the non-stale model updates with different data recovery methods, measured by 1-cosine similarity

The most commonly used approach to recovering the training data from a trained ML model involves training an extra generative model, to compel its generated data samples to exhibit high predictive value on the original model [42], and to add image prior constraint terms to enhance data quality [21]. On the other hand, data recovery can also be achieved by directly optimizing randomly initialized input data until it performs well on the original model [34]. However, the results of our preliminary experiments, using the LeNet model and the MNIST dataset, show that none of these approaches can provide good quality of the computed data, in order to be used in our FL scenarios.

More specifically, these existing approaches can ensure that the computed dataset, as a whole, exhibits some characteristics of the original training data. For example, as shown in Figure 20, the averaged image of the recovered data samples in each data class can resemble a meaningful image that matches the data pattern in the original dataset. However, the individual image samples being computed have very low quality. If these computed data samples are used to compute the non-stale model updates in FL, it will result in a significant error in estimating the non-stale model updates, which greatly exceeds the error produced by our proposed gradient inversion (GI) based estimation, as shown in Table 6.

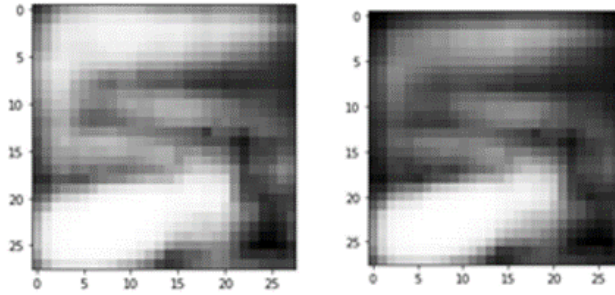


Figure 21: Two computed image samples in class 5 of the MNIST dataset

Furthermore, as shown in Figure 21, the computed data samples lack diversity, resulting in high similarity among the generated samples in the same data class. Training on such highly similar data samples can easily lead the model to overfit.

Some attempts have been made to enhance the data quality by incorporating another extra public dataset to introduce general image knowledge [30], but the effectiveness of this approach highly depends on the specific choice of such public dataset. Experimental results in [1] demonstrate that the quality of computed data can only be ensured if the extra public dataset shares the similar data pattern with the original training dataset. For example, in our preliminary experiments, we selected CIFAR-100 as the public dataset, and the original training datasets included CIFAR-10 and SVHN datasets. As shown in Figure 22, when CIFAR-10 is used as the training dataset, the computed data exhibits higher quality compared with that using the SVHN dataset as the training dataset, because the CIFAR-10 dataset shares the similar image patterns with the CIFAR-100 dataset.

Because of such low quality of the computed data, they cannot be directly used to retrain the global model in FL, as an estimate to non-stale model updates. Some existing approaches, instead, use knowledge distillation to transfer the knowledge contained in the computed data to the target ML model [6, 42]. However, in our FL scenario, since the server only conducts aggregation of the received clients' model updates and lacks the corresponding test data (as part of the clients' local data), the server will be unable to decide if and when the model retraining will overfit (Figure 23). Furthermore, all the existing methods require that the clients' model updates have to be fully trained, but this requirement generally cannot be satisfied in FL scenarios.

Compared to the existing methods, our proposed technique uses gradient inversion to obtain an estimation of the clients' original training data. Since we only require the computed data to mimic the model's gradient produced with the original training data, we do not necessitate the quality of



Figure 22: The computed data samples from different training datasets

individual data samples being computed, and could hence avoid the impact of the computed data's low quality on the FL performance.

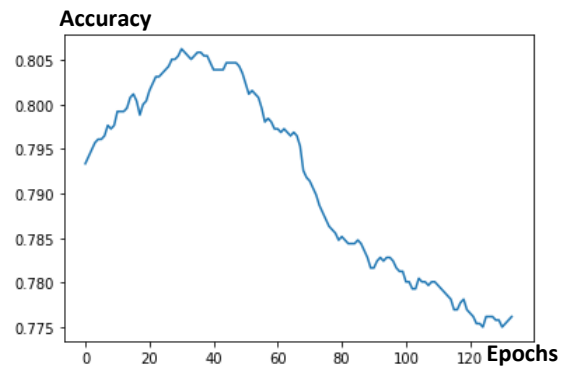


Figure 23: The knowledge distillation, when being applied to retrain the global model in FL, will overfit after a specific number of epochs